

# Study on drying performance of high voltage cable buffer layer material

Jing Zhang<sup>1,\*</sup>, Jinghua Liu<sup>2</sup>, Chuanxian Luo<sup>1</sup>, Liang He<sup>3</sup>, Lifeng Cheng<sup>1</sup>, and Yuru Cai<sup>1</sup>

<sup>1</sup>Wuhan Nari Limited Liability Company of State Grid Electric Power Research Institute Wuhan, China

<sup>2</sup>State Grid Corporation of China Beijing, China

<sup>3</sup>Shenzhen Power Supply Bureau Co., Ltd. Shenzhen, China

**Abstract.** In order to study the failure mechanism of high-voltage cable buffer layer caused by moisture and the performance of the material after immersion and drying, according to the structure and size of 110 kV XLPE cable, the requirements for the separation distance between corrugated aluminum sheath and insulating outer shield before and after the change of buffer layer resistivity caused by moisture were calculated, the influence of moisture on ablation failure was analyzed. The test platform of buffer layer material was built, the properties of two kinds of materials without water immersion and after water immersion drying were tested, including semi-conductive buffer water-blocking tape and semi-conductive buffer tape. The results show that when the moisture content was large, the resistivity of the buffer layer increases, which reduces the requirements of the allowable separation distance of the cable, and was more likely to cause the discharge and ablation of the buffer layer. The water in the buffer layer was removed by drying at 70 °C, with thickness, weight, the water content, elongation at break, breaking strength and volume resistivity can be recovered, which verifies that the heating drying method is feasible for the removal of water from the buffer layer.

**Keywords:** Cable; Buffer layer; Ablation; Water content; Drying process.

## 1 Introduction

XLPE cable with buffer layer and corrugated aluminum sheath structure is widely used in underground transmission lines<sup>[1-4]</sup>. At present, the buffer layer mainly has two structures of semi-conductive buffer tape and semi-conductive buffer water-blocking tape. The semi-conductive buffer tape is usually composed of one or more layers of semi-conductive non-woven fabric, and the semi-conductive buffer water-blocking tape is mainly composed of a layer of semi-conductive non-woven fabric, a layer of semi-conductive fluffy cotton, and a layer of polyacrylate expansion powder pasted in the middle. The polyacrylate swelling powder can expand rapidly in contact with water, thereby preventing the water from spreading longitudinally along the cable when the corrugated aluminum sheath is defective.

---

\* Corresponding author: narizhangjing@foxmail.com

In recent five years, there have been many ablation and breakdown failures of buffer layer of high voltage cable in China, which have attracted the attention of relevant departments and researchers. There are two main features of the fault, there are ablation marks at the corresponding positions of the insulating shield, buffer layer and corrugated aluminum sheath, in addition, white substances are precipitated inside the buffer layer<sup>[5-6]</sup>. The ablation of cable buffer layer has been widely discussed, including failure mechanism, influencing factors and detection methods<sup>[7-9]</sup>. However, due to improper storage or improper laying process of the cable, after the corrugated aluminum sheath is damaged, the humidity inside the layer will change greatly, causing the cable buffer layer ablation failure, so the dry repair method is very important.

In this paper, the ablation mechanism of cable buffer layer affected by moisture and water is analyzed, the buffer layer test platform is built, and weight, thickness, volume resistivity, fracture strength, fracture elongation and moisture content of the buffer layer material before wetting and after wetting and drying are studied. The research conclusions can provide a basis for the treatment of cable buffer layer after water immersion.

## 2 Mechanism of Water Induced Ablation of Buffer Layer

In order to analyze the surface ablation along the axial length of the cable caused by moisture, according to the paper<sup>[9]</sup>, the cable buffer layer and the insulating shielding layer were equivalent to a "composite layer", and an equivalent circuit of high-voltage cable axial ablation along the surface was established, and the requirements for the separation distance between the cable metal sheath and the insulating outer shielding when the cable was discharged was deduced, see (1). Among them,  $d_1$  is the outer diameter of the conductor shielding layer;  $d_2$  is the outer diameter of the insulating layer;  $\delta$  is the thickness of the composite layer;  $D$  is the average diameter of the composite layer,  $D=d_2+2\delta$ ;  $2L$  is the allowable contact distance between corrugated aluminum sheath and composite layer, and the unit is mm.

$$L \leq \sqrt{\frac{1.8 \times 10^{12} U_s \delta (d_2 + \delta) \ln(d_2 / d_1)}{f U_0 \epsilon \rho}} \quad (1)$$

It should be noted that (1) is used to describe the capacitive current  $I$  in the distance  $2L$  between two points where the corrugated aluminum sheath is in close contact flows into the corrugated aluminum sheath axially along the composite layer, causing partial potential increase between two points. It can be seen from (1) that the allowable separation pitch  $L$  is proportional to the thickness  $\delta$  of the composite layer and the allowable longitudinal voltage  $U_s$ , and is inversely proportional to the dielectric constant  $\epsilon$  of the XLPE material, the resistivity  $\rho$  of the composite layer and the operating voltage  $U_0$ .  $U_s$  is the allowable longitudinal voltage.

The study showed that the volume resistivity of the buffer layer material increased when it was damp, and the resistivity of the buffer layer after damp was increased by about 0.5 times. After immersion in water, the volume resistivity of the buffer layer material can be increased by 10000 times. In order to study the influence of volume resistivity of buffer layer material on axial surface ablation after immersion, this paper took 110 kV 630 mm<sup>2</sup> XLPE cable structure as an example to calculate the allowable separation distance under different composite layer resistivity. The specific parameters of the cable are as follows: the diameter of the conductor is 30 mm; the diameter of the conductor shielding layer is 32.8 mm; the outer diameter of the insulating layer is 65.8 mm; the inner diameter of the corrugated aluminum sheath is 75.8 mm; the dielectric constant of the XLPE insulating material is 2.3, and the phase voltage  $U_0$  is 64 kV. The allowable longitudinal voltage  $U_s$  is

set to 100V, the thickness of the composite layer is 3 mm, and the parameters were substituted into (1) to calculate the relationship between the resistivity of the composite layer and the allowable pitch of the cable, as shown in Fig.1.

It can be seen from the Fig.1 that the increase of the resistivity of the composite layer will reduce the requirement for the cable to allow the separation distance of 2L, making the axial ablation of the buffer layer easier. When the resistivity is  $10^2 \Omega \cdot \text{cm}$ , the allowable separation distance is 1186 cm, and axial creeping discharge is not easy to occur. When the resistivity reaches  $10^6 \Omega \cdot \text{cm}$  due to immersion in water, the allowable separation distance of the cable is 11.86 cm. If this distance is exceeded, axial creeping discharge will occur, resulting in the ablation of the buffer layer.

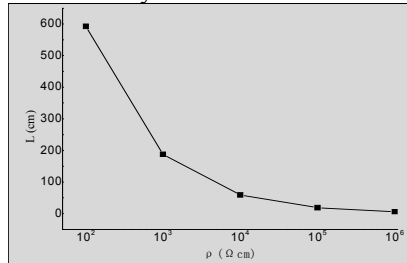
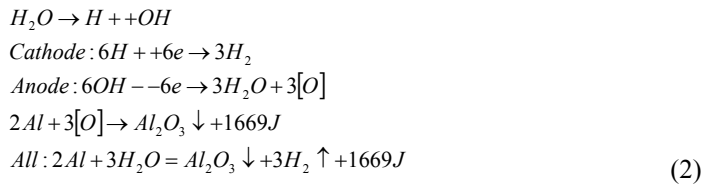


**Fig. 1.** The relationship between the resistivity of the composite layer and the allowable pitch of the cable

In addition to increasing the probability of partial discharge, the moisture in the buffer layer could also participate in the electrocorrosion reaction of the corrugated aluminum sheath<sup>[10]</sup>. The specific process is as follows:



Ouyang benhong et al.<sup>[11]</sup> also verified through experiments that the damp buffer layer generated white material containing  $Al_2O_3$ , and the white product was a non-conductive material, which would lead to poor local contact between the aluminum sheath and the insulation shield, and further induced the buffer layer to ablate and caused cable faults.

### 3 Sample Immersion Treatment and Experimental Method

#### 3.1 Test samples

Four samples of two types, 1# and 3# are semi-conductive buffer water-blocking tapes, 2#, 4# are semi-conductive buffer tapes, Fig. 2 was given. Among them, 1# and 3# samples are thicker, and the upper and lower surfaces are compact and smooth, while the upper and lower surfaces are loose and rough, 2# and 4# are thin, and the upper and lower surfaces are compact and smooth. Samples from different manufacturers.



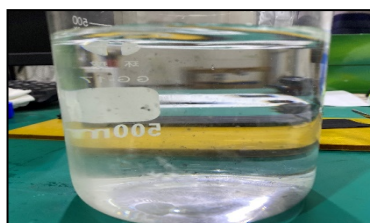
**Fig. 2.** Test sample

### 3.2 Treatment of water invasion

Considering that the direct penetration of liquid water into the cable buffer layer was the most serious, four buffer layer samples were cut to pieces of the same size (2cm×2cm). Hold it in water with tweezers for several seconds. During immersion, it was found that semi-conductive buffer water-blocking tapes rapidly absorbed and expanded after being immersed in water, and crystallization had occurred in the intermediate layer. When they were soaked for 3s, two thinner tapes appeared, and slight semi-conductive powders appeared in the water as shown in Fig. 3 (a), (b). When soaked for 5s, severe stratification occurred, and a large number of semi-conductive powders were dissolved in water as shown in Fig. 4 (a), (b).



(a) sample

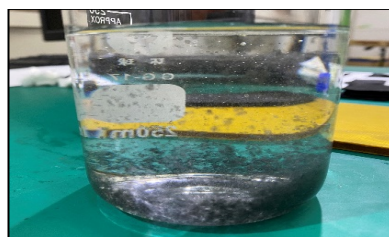


(b) powders in water

**Fig. 3.** 1#, 3# sample soaking for 3s



(a) sample



(b) powders in water

**Fig. 4.** 1#, 3# sample soaking for 5s

The occurrence of powder falling or stratification means that the structure was damaged. The measurement of such samples is of little significance because their structure has changed. Therefore, the immersion time shall be strictly controlled in the test, ensure that the structure of four samples was not damaged. Through the experiment, all samples were soaked for 2s, the water can be fully absorbed, and there was not obvious semi-conductive powder residue in the water. In addition, the time of structural damage of the sample immersed in water may be related to the size of the tape sample. Therefore, for the sample actually submitted for inspection, the immersion time needs to be determined according to its size.

### 3.3 Drying process

In practical engineering, the method of vacuumizing one end of the cable and filling one end with nitrogen is often used to realize the water drive and drying of the cable. Considering that this method is not suitable for drying the buffer layer materia in the laboratory, therefore, the oven drying method was adopted. Samples were placed in an oven at a temperature of 70 °C. The samples were taken out every 10 minutes and weighed, until the quality of the samples was equal two times. The samples were considered to have been completely dried and the time for each sample to be fully dried was recorded. The drying time of samples was related to the size. For four samples of 2cm×2cm, the complete drying time was 2 h, and for samples of 65cm length, the oven was dried at 70 °C for 4 h.

### 3.4 Test methods

In order to explore the influence of drying after wetting on the mechanical and electrical properties of four tapes of cable buffer layer, six parameters were tested by referring to the test method of JB/T 10259-2014 buffer water-blocking tape for cable and optical cable.

## 4 Test and analysis

### 4.1 Weight

Weight refers to the quality of the water-blocking tape per square meter, the unit is  $g/m^2$ , which should be measured in accordance with GB/T 451.2. The sample area is 50,000  $mm^2$  and the number of samples should not be less than 5. When preparing specimens, five samples were stacked vertically along the sheet of paper, and then two layers of 0.01  $m^3$  specimens were evenly cut along the transverse direction. A total of 10 specimens were used to measure the weight before and after immersion using a scale. Fig.5 presents the measurement result.

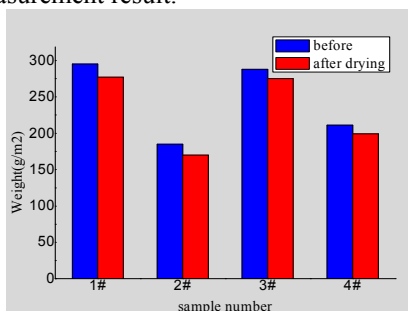


Fig.5. Weight of samples before and after drying

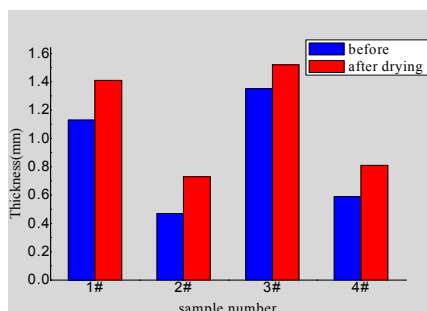


Fig.6. Thickness of samples before and after drying

The weight of the four buffer layers was lower than before wet drying. The weight with immersion drying treatment was reduced by 6.1%, 8.1%, 4.5% and 5.7% compared with that before treatment, respectively. The weight change before and after the treatment of 2# was the largest, while the change of 3# was the smallest.

### 4.2 Thickness

Thickness refers to the distance between the upper and lower sides of the buffer water-

blocking tape, the unit is mm, measured according to GB/T 451.3. Fig. 6 shows the result of the measurement.

The thickness of the four buffer layer samples was increased compared with that before wet drying. The thickness of 1#~4# specimens treated by immersion drying increased by 24.8%, 55.3%, 12.6% and 37.3% compared with that before treatment, respectively. The thickness change before and after 2# treatment was the largest, while 3#change was the smallest.

### 4.3 Volume resistivity

Volume resistivity is the ratio of DC voltage to steady-state current in a material. The unit is  $\Omega \cdot \text{cm}$ . Three samples were prepared according to GB/T 450. The sample was placed on a copper plate electrode during measurement, and then a copper electrode was pressed on the sample. Between the two electrodes 4.5V DC voltage was applied. After charging for 1 min, the measured volume resistance value was read by a multimeter. The volume resistivity changes of the four buffer layers before and after wet drying were shown in Fig. 7.

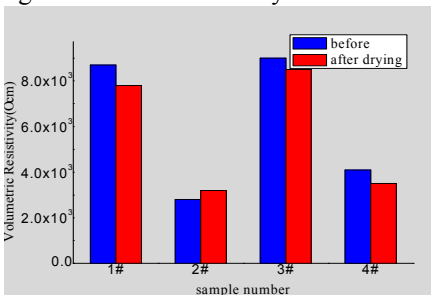


Fig. 7. Volume resistivity of samples drying

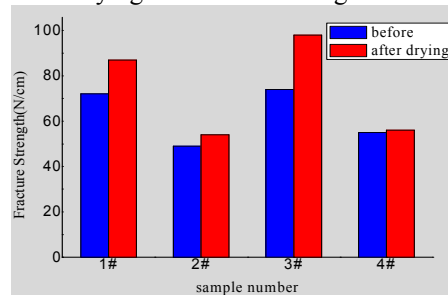


Fig. 8. Fracture Strength of Samples

The technical requirement of the volume resistivity of the semiconductive buffer water-blocking tape given in JB/T 10259-2014 "Water-blocking tape for cables and optical cable" is  $\leq 1 \times 10^5 \Omega \cdot \text{cm}$ . The volume resistivity before and after the four buffer layers treatment meets the technical requirements. The Volume resistivity of 1#~4# have changed by -10.3%, 14.3%, -5.6% and -14.6% compared with that before treatment, respectively.

### 4.4 Fracture Strength

Fracture strength refers to the ratio of the pull force to the length of the fracture cross-section at the time of the breaking of the sample, the units is N/cm. According to GB/T 12914. The change of fracture strength of four buffer layer materials before and after wet drying was shown in Fig. 8.

The technical requirements for fracture strength of semi-conductive water-resisting belts given in JB/T 10259-2014 is  $\geq 40 \text{ N/cm}$ ). The fracture strength before and after treatment of four samples meet the technical requirements, and the fracture strength was increased compared with that before treatment. The fracture strength of 1#~4# samples was increases by 20.8%, 10.2%, 32.4% and 1.8% respectively compared with that before treatment. The fracture strength of 3# increased the most, 4# increased the least.

### 4.5 Fracture elongation

Fracture elongation is the ratio of the elongation of the specimen to the length before tension when the specimen was subjected to external forces until it breaks. The test method

was in accordance with GB/T 12914. The test data was shown in Fig. 9.

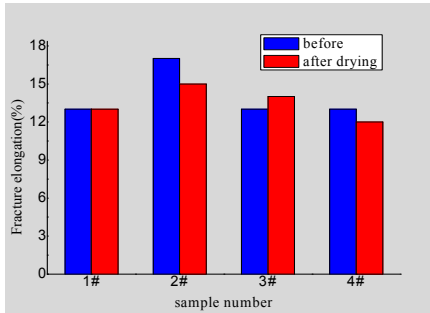


**Fig. 9.** Fracture elongation of samples

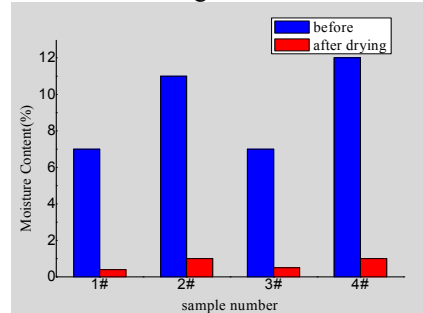


**Fig. 10.** Moisture content of samples

The technical requirements for the fracture elongation of sample given in JB/T 10259-2014 is <12%. The fracture elongation before and after treatment of the samples meet the technical requirements. The longitudinal breaking elongation of 1#-4# changed 0, -11.8%, 7.7% and -7.7% respectively compared with that before treatment.

### 4.6 Moisture Content

Moisture content refers to the difference between the water weight and the dry weight of the sample divided by the percentage of the water weight. Perform the test according to the method specified in GB/T 462. First, weigh the quality of the sample and the sample container before drying, then put the container containing the sample into an oven which can keep the temperature at  $105^{\circ}\text{C}\pm 2^{\circ}\text{C}$ . When drying, the lid of the container was opened, cover the container quickly after drying, the lid of the container immediately after cooling was opened, so that the air pressure inside and outside the container was equal, and then weigh the container containing the sample. The quality of the sample was calculated. When the difference in weighing is not more than 0.1% of the sample mass before drying, Calculated the moisture content.

The moisture content of all four buffer layers decreased by 90% - 95% after Wet-Drying treatment, and the moisture content was below 1% (JB/T 10259-2014 requires less than 7%) with a higher drying degree.

## 5 Conclusion

In this paper, the effect of buffering layer immersion on axial ablation fault of high voltage cable is analyzed. The changes of physical and chemical properties, mechanical properties and electrical properties of buffering layer after immersion are experimentally studied, the conclusions are as follows:

(1) The thickness of the buffer layer sample increase compared with that before drying, and weight decrease. Volume resistivity, fracture strength and fracture elongation before and after drying meet the technical requirements specified in JB/T 10259-2014, and the fracture strength after soaking and drying are increased compared with before. The moisture content can reach below 1% after being wetted and dried.

(2) The moisture in buffer layer is removed by drying at  $70^{\circ}\text{C}$ . The influence on mechanical and electrical properties of buffer layer is basically within control range, which verifies that it is feasible to use heating drying method to remove water in buffer layer. However, for the water immersed buffer layer, it no longer has the function of blocking water after water removal.

## References

1. Wang Wei, Zhang Jing, Zheng Jiankang, Ouyang Benhong. Effect of steep wave process on breakdown characteristics of intermediate joint during closing [J]. *Wire & Cable*, 2018 (05): 26-31.
2. Fu Fangda, Yang Xu, Pan Cheng, Yao Yuhang, Jiang Yi, Zhang Jing, Wang Luliang. Identifying insulation defects of XLPE cable with suppressing the influence of PD aging [J]. *Electrotechnics Electric*, 2020 (04): 16-24.
3. Zhang Jing, Cheng Lin, song Pengxian, Liu Jiping, Wang Wei. Analysis on thermal state of high voltage cable terminal based on silicone oil degradation characteristics [J]. *Insulating Materials*, 2020,53 (03): 89-93.
4. P. Song,Z. Meng, X. Li, M. Zhu, Y. Yu and S. Fang, "A Case Study on Ablation Breakdown of High Wall Cable Buffer Layer," 2020 IEEE International Conference on High V Engineering and Application (ICHVE), 2020, pp. 1-4.
5. Li Chenying, Li Hongze, Chen Jie, et al. Analysis of buffer layer discharge problem of high voltage XLPE power cable[J]. *Electric Power Engineering Technology*, 2018, 37(2):61-66.
6. CHARLES Q S. Failure analysis of three 230 kV XLPE cables[C]//2010 IEEE/PES Transmission and Distribution Conference and Exposition, Latin America: 22-25.
7. Chen Zhiyong,Zhang Jing. Discharge characteristics of buffer layer of 110 kV XLPE power cables with different cross sections[J]. *Cable technology*, 2014 (3): 1-5.
8. Chen Zhiyong,Zhang Jing. Discharge characteristics of metal sheath and insulation shield of high voltage XLPE cable[J]. *Cable technology*, 2013 (3): 3-9.
9. Zhang Jing, Wang Wei, Xu Mingzhong, song Pengxian, Li Wenjie, Ouyang benhong. Mechanism analysis of axial surface ablation failure of buffer layer of high voltage cable [J]. *Power engineering technology*, 2020,39 (03): 180-184.
10. Wang Wei, Ouyang benhong, Xu Mingzhong, Zhang Jing, Yan Youxiang. Preliminary analysis of ablation of cable buffer layer [J]. *Wire and cable*, 2019 (05): 5-10.
11. Ouyang benhong, Li Wenjie, Liu Ying, Lian Rui. Ablation Mechanism of Water-blocking Buffer Layer in HV XLPE Cables [J]. *High Voltage Engineering* , 2021, 47 (09): 3153-3162.